JACS
JOURNAL OF THE AMERICAN CHEMICAL SOCIETY
Article
pubs.acs.org/JACS

Distortion-Controlled Reactivity and Molecular Dynamics of Dehydro-Diels–Alder Reactions

Peiyuan Yu,[†] Zhongyue Yang,[†] Yong Liang, Xin Hong, Yanwei Li, and K. N. Houk*

Department of Chemistry and Biochemistry, University of California, Los Angeles, California 90095, United States

Supporting Information

ABSTRACT: We report density functional theory (M06-2X) studies of a series of dehydro-Diels–Alder (DDA) reactions. For these and the parent reaction, the stepwise mechanisms have similar barriers, whereas the barriers of the concerted mechanisms differ significantly. The reactivity of DDA reactions is controlled by distortion energy. The concerted and stepwise mechanisms of the hexadehydro-Diels–Alder (HDDA) reaction are competitive with activation barriers of ~36 kcal/mol. This is because a large distortion energy (~43 kcal/mol) is required to achieve the concerted transition state geometry. MD simulations reveal that productive concerted trajectories display a strong angle bending oscillation (~25° oscillation amplitude), while the stepwise trajectories show only a chaotic pattern and less pronounced bending vibrations.

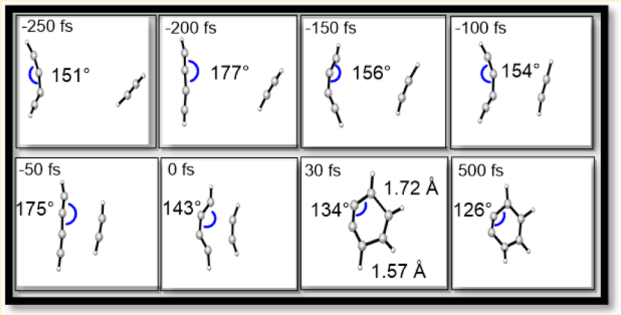

INTRODUCTION

The Diels–Alder (DA) reaction between a diene and a dienophile (alkene or alkyne) represents one of the most widely utilized and well-studied synthetic transformations in organic chemistry (Scheme 1, eqs 1 and 2).[1−5] This (4 + 2) cycloaddition is particularly useful for constructing six-membered rings with up to four stereogenic centers in a single step, often with good regio- and stereocontrol. Various aspects of the DA reactions, such as mechanism,[6] dynamics,[7] selectivity,[8] asymmetric catalysis,[9] and industrial applications,[10] have attracted generations of theoretical and synthetic chemists ever since its original discovery in 1928.[1] Specific types or variants of DA reactions, such as intramolecular (IMDA) and transannular (TADA) reactions,[11−14] and hetero-Diels–Alder (HDA) reactions,[15,16] have been categorized. Novel utilities and new aspects of DA reactions are still emerging. The development of the tetrazine ligation[17−19] (an inverse electron demand HDA reaction[20] widely used for bioorthogonal applications) and the search for enzymes that catalyze DA reactions (Diels–Alderases)[21−23] are recent examples.

Scheme 1. Diels–Alder (DA) and Dehydro-Diels–Alder (DDA) Reactions

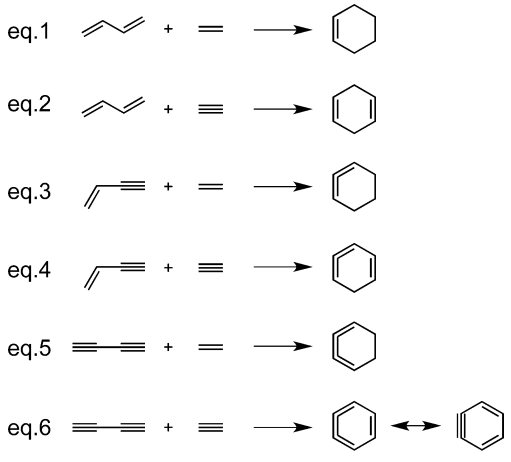

In 2008, Wessig et al. described another important variant of the DA reaction, the dehydro-Diels–Alder (DDA) reaction[24] (Scheme 1, eqs 3–6). If one or both double bonds in the diene component of a DA reaction are replaced by a triple bond, the product must contain cumulated double bonds (i.e., cyclic allenes).[25] Due to high strain, these initially formed species usually undergo further reactions such as hydrogen migration or dimerization to generate more stable final products.[24] The trapping of these reactive intermediates in a controlled fashion was the key to harnessing the synthetic power of DDA reactions. Over the past few years, various research groups have demonstrated the synthetic utility of DDA reactions.[26−29] One prominent example of these achievements is the development of the intramolecular version of eq 6 (Scheme 1), the hexadehydro-Diels–Alder (HDDA) reaction.[30]

Mechanistically, thermal DA reactions are symmetry allowed pericyclic transformations according to Woodward–Hoffmann rules.[31] In most cases, they are concerted processes, although stepwise mechanisms via diradical intermediates operate in some special cases.[24] However, for HDDA reactions, whether the reactions are concerted or stepwise has engendered some

Received: April 28, 2016
Published: June 10, 2016

DOI: 10.1021/jacs.6b04113
J. Am. Chem. Soc. 2016, 138, 8247–8252

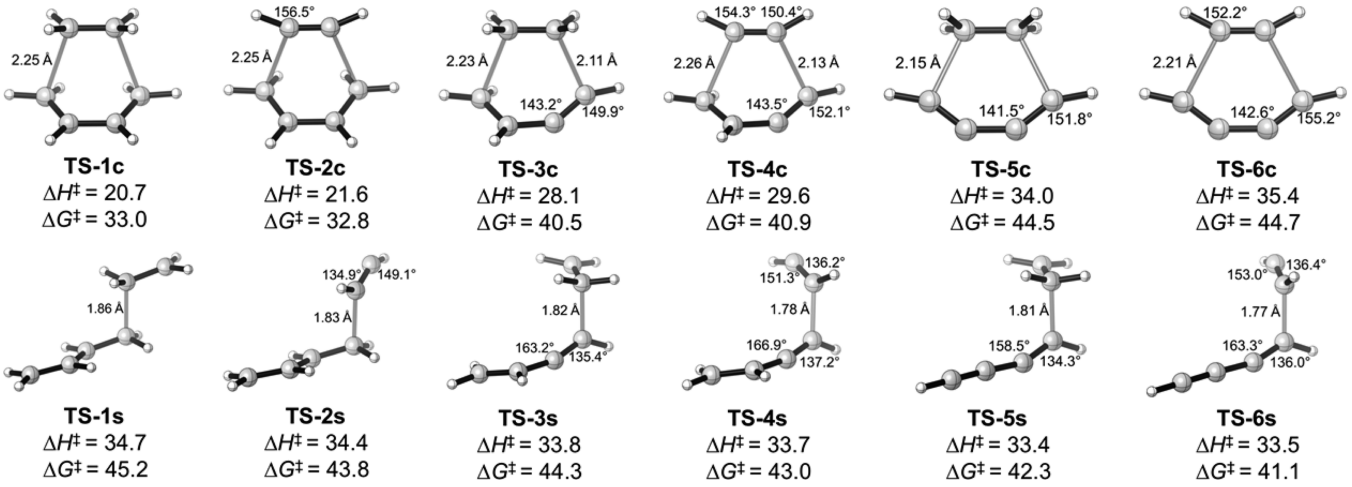

Figure 1. (U)M06-2X/6-311+G(d,p)-optimized transition structures for the concerted and stepwise DA and DDA reactions. Enthalpies and free energies of activation are in kcal/mol.

controversy recently. Schaefer et al. studied the thermal fragmentation of *ortho*-benzyne (a retro-HDDA reaction), a process that is believed to play an important role in the combustion of aromatic compounds.[32] According to *ab initio* calculations, the concerted mechanism is consistent with experimental observations. However, it was pointed out "there may also be a competitive, nonconcerted route through an open-chain singlet diradical intermediate, a problem that awaits elucidation".[32] In 2011, Johnson et al. reported (U)CCSD(T)//M05-2X computational results on the concerted and stepwise pathways for all six reactions shown in Scheme 1.[33] It was found that a concerted reaction is favored in every case, but the difference between the barriers of the two mechanisms is only 0.5 kcal/mol for the last reaction (eq 6).[33] Recently, Cramer, Hoye, and Kuwata reported a combined experimental and computational study of intramolecular HDDA reactions.[34] They found that the stepwise transition states are lower in energy than the corresponding concerted ones, and the computed barriers of reaction are in good agreement with experimentally measured kinetics. While the stepwise mechanism is most likely involved in the intramolecular HDDA reactions of substituted reactants, there is competition between concerted and stepwise mechanisms for the parent reaction (eq 6). Johnson et al. showed that for the series of DA and DDA reactions in Scheme 1, the advantage of the concerted mechanism diminishes as the substrate becomes more unsaturated.[33] Our group has studied computationally the mechanism of bimolecular HDDA reactions involving substituted substrates.[35] We found that the accelerating effect of alkynyl substituents on the reaction rate is due to the decrease in distortion energy required to achieve the stepwise transition states. Very recently, Hoye and co-workers reported another intriguing type of DDA reactions, the pentadehydro-Diels–Alder (PDDA) reaction.[36] The PDDA reactions are also likely involving stepwise mechanisms according to density functional theory (DFT) calculations.[36]

These results prompted us to ask how distortion energies contribute to the increase in concerted barriers for DA and DDA reactions. We have now conducted DFT studies and performed distortion/interaction analyses on the 6 DA and DDA reactions shown in Scheme 1. We also performed direct molecular dynamics (MD) simulations on HDDA reactions, to illuminate how reactants distort into transition state geometries in both concerted and stepwise trajectories.

COMPUTATIONAL METHODS

All density functional theory (DFT) computations were performed using Gaussian09.[37] Geometry optimizations were carried out at the (U)M06-2X/6-311+G(d,p) level of theory.[38] HOMO–LUMO mixing for the initial guess was used for open-shell singlet calculations. Normal vibrational mode analysis at the same level confirmed that optimized structures were minima or transition states (TS). The distortion/interaction analysis is based on "electronic energies (*E*)", which are the energies of hypothetically rigid molecules. This is used, instead of *H* or *G*, because the distorted separated fragments are not stationary points and no harmonic frequency analysis can be performed to obtain *H* and *G*.

(U)M06-2X/6-31G(d) was found to give qualitatively the same conclusions about the relative energetics of the reactions studied. Therefore, molecular dynamics (MD) simulations were performed at the (U)M06-2X/6-31G(d) level of theory. Direct molecular dynamics (MD) simulations were performed for the concerted and stepwise reactions of diyne–yne (Scheme 1, eq 6) in the gas phase. Quasiclassical trajectories (QCTs) were initialized in the region of the potential energy surface near the TS. Normal mode sampling involved adding zero-point energy for each real normal mode in the TS, and performing a Boltzmann sampling of geometries to afford the thermal energy available at 300 K with a random phase. (The distribution of sampled transition state geometries is shown in overlays in Figure S1.) The trajectories were propagated forward and backward, 500 fs in each direction. The classical equations of motion were integrated with a velocity-Verlet algorithm using Singleton's program Progdyn,[39] with the energies and derivatives computed on the fly by the UM06-2X method using Gaussian 09. The step length for integration was 1 fs.

RESULTS AND DISCUSSION

The top row of Figure 1 shows the six transition structures **TS-1c–6c** for the concerted reactions. For the stepwise reactions, the transition structures **TS-1s–6s** for the formation of diradical intermediates are shown in the bottom row of Figure 1. The enthalpies and free energies of activation for the concerted and stepwise reactions are shown below the corresponding TS. The concerted mechanisms are energetically favored over the stepwise mechanisms for eqs 1–4. In contrast, **TS-5s** and **TS-6s** are lower in energy than **TS-5c** and **TS-6c**, respectively. The detailed energetics for all six reactions are summarized in Tables 1 and 2. These are electronic energies,

DOI: 10.1021/jacs.6b04113
J. Am. Chem. Soc. 2016, 138, 8247–8252

Table 1. Activation, Distortion, Interaction, and Reaction Energies (in kcal/mol) Calculated with M06-2X/6-311+G(d,p) for Concerted Reactions

entry	TS	E_{act}	$E_{dist\text{-}4\pi}$	$E_{dist\text{-}2\pi}$	E_{dist}	E_{int}	E_{rxn}
1	**TS-1c**	19.6	18.8	7.4	26.1	−6.5	−47.6
2	**TS-2c**	21.2	17.1	10.3	27.4	−6.2	−61.8
3	**TS-3c**	27.3	24.3	10.6	34.9	−7.6	−18.6
4	**TS-4c**	29.5	22.2	14.0	36.2	−6.7	−30.0
5	**TS-5c**	33.9	32.8	11.4	44.3	−10.4	−4.4
6	**TS-6c**	36.0	29.2	14.0	43.2	−7.2	−57.3

Table 2. Activation, Distortion, and Interaction Energies (in kcal/mol) Calculated with (U)M06-2X/6-311+G(d,p) for Stepwise Reactions[a]

entry	TS	E_{act}	$E_{dist\text{-}4\pi}$	$E_{dist\text{-}2\pi}$	E_{dist}	E_{int}	$E_{(DR)}$	$E_{(TSs2)}$
1	**TS-1s**	35.4	12.6	12.2	24.9	10.5	28.5	32.1
2	**TS-2s**	35.4	10.9	16.5	27.4	8.0	27.0	29.1
3	**TS-3s**	34.5	13.5	11.2	24.7	9.8	27.8	32.9
4	**TS-4s**	35.0	11.9	15.1	27.0	8.0	25.0	28.3
5	**TS-5s**	34.2	14.8	11.0	25.8	8.4	29.5	37.8
6	**TS-6s**	35.2	13.0	14.6	27.5	7.7	25.7	30.8

[a]Energies of diradical intermediates (DR) and second transition state (TSs2) are also shown.

including no ZPE or thermal corrections, so that the distortion energies can be evaluated. The activation energies and reaction energies agree qualitatively with Johnson's results.[33] For the concerted pathways (Table 1), the barriers of reaction (E_{act}) range from 19.6 to 36.0 kcal/mol for the six reactions. In contrast, for the stepwise pathways (Table 2), transition states **TS-1s**−**6s** are very close in energy relative to the corresponding reactants (34.2−35.4 kcal/mol). The first steps are rate-determining except for the reaction between diyne and ene (entry 5), where the second TS (37.8 kcal/mol) is 3.6 kcal/mol higher in energy than the first TS (34.2 kcal/mol). This might be due to the instability of the product of ring closure, the cyclic cumulene (E_{rxn} = −4.4 kcal/mol, Table 1, entry 5). In fact, the diradical would prefer to form a cyclobutene (in a [2 + 2] cycloaddition) instead of cyclic cumulene. Comparing the E_{act} values in Table 1 to those of Table 2 for all six reactions, it is clear that the preference for concerted mechanism diminishes as the reaction goes from DA (eq 1) to HDDA (eq 6). For the HDDA reaction, **TS-6s** is 0.8 kcal/mol lower in energy than that of **TS-6c**.

Both concerted and stepwise transition states (**TS-1c**−**6c** and **TS-1s**−**6s**) were analyzed using the distortion/interaction model,[40] also known as the activation strain model.[41] For each reaction, the transition structure is separated into two fragments (diene/enyne/diyne and ene/yne), followed by single-point energy calculations on each fragment. The difference in energy between the distorted fragments and optimized ground-state geometries is the distortion energy of diene/enyne/diyne ($E_{dist\text{-}4\pi}$) and ene/yne ($E_{dist\text{-}2\pi}$), respectively. The difference between the activation energy (E_{act}) and the total distortion energy ($E_{dist} = E_{dist\text{-}4\pi} + E_{dist\text{-}2\pi}$) is the interaction energy (E_{int}). The results are also shown in Tables 1 and 2.

For concerted reactions (Table 1), distortion energies are the main contributors (26−44 kcal/mol) to the activation barriers, while the favorable (negative) interaction energies are relatively small (−6 to −10 kcal/mol). For each reaction, the distortion energy of the 4π component ($E_{dist\text{-}4\pi}$) is the main contributor to the total distortion energy, because significant bending distorts the planar or linear molecule into the concerted transition state geometry, where both termini of the diene/enyne/diyne overlap with the termini of the ene/yne. In contrast, for the stepwise reactions (Table 2), the $E_{dist\text{-}4\pi}$ and $E_{dist\text{-}2\pi}$ are similar in magnitude and approximately constant at 11−16 kcal/mol each. In the stepwise transition states, the 4π components distort much less than in the concerted transition states. Nevertheless, the total distortion energies are still the controlling factors of activation barriers, whereas the unfavorable (positive) interaction energies are relatively small as well (8−10 kcal/mol). We previously demonstrated that alkynyl substituents accelerate the HDDA reaction by ∼5 orders of magnitude, mainly by decreasing the distortion energy required to achieve the diradical transition state.[35] In the present study, the distortion energy still predominantly influences the reactivity of unsubstituted DA and DDA reactions. Most notably, the great difference in activation energies (E_{act}) for the six concerted reactions is associated with the dramatic change in distortion energies (E_{dist}). Generally, reaction with a higher E_{dist} tends to have a higher E_{act}, except for the reaction between diyne and ene (Table 1, entry 5), in which the interaction energy (−10.4 kcal/mol) partially offsets the highest distortion energy (44.3 kcal/mol). This trend is illustrated in Figure 2,

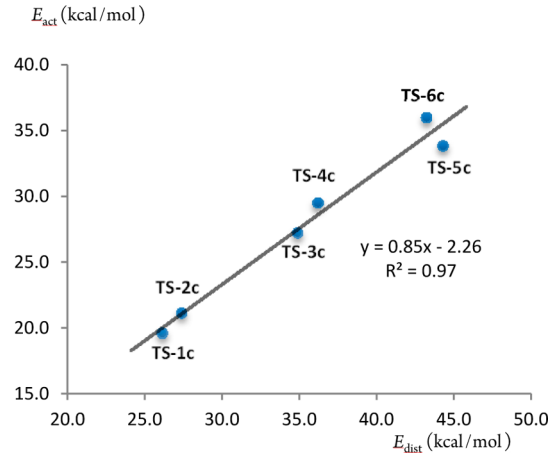

Figure 2. Plot of activation energies versus distortion energies for six concerted reactions. Energies are in kcal/mol.

which is a plot of E_{act} versus E_{dist} for the six concerted reactions. One manifestation of this trend is that, for the HDDA reaction, the stepwise mechanism becomes competitive, whereas for DA reactions, the concerted mechanisms are energetically favored. The high barrier of the concerted mechanism for the HDDA reaction is attributed to the high distortion energy required to distort the reactants into transition state geometries.

We performed direct molecular dynamics (MD) simulations for the concerted and stepwise mechanisms of the diyne−yne (HDDA) reaction to study how reactants distort into transition state geometries in a time-resolved fashion. In particular, the vibrations that must be excited for reaction to occur are of special interest. Figure 3 shows snapshots of two typical reactive trajectories in butadiyne−acetylene cycloadditions, a prototype of HDDA reactions. Figure 3a,b are two trajectories, one for a concerted and the other for a stepwise pathway, respectively. The bond angles and time at which each snapshot is taken are shown for eight snapshots of each trajectory. As shown in Figure 3a, a strong bending motion is observed for butadiyne

DOI: 10.1021/jacs.6b04113
J. Am. Chem. Soc. 2016, 138, 8247−8252

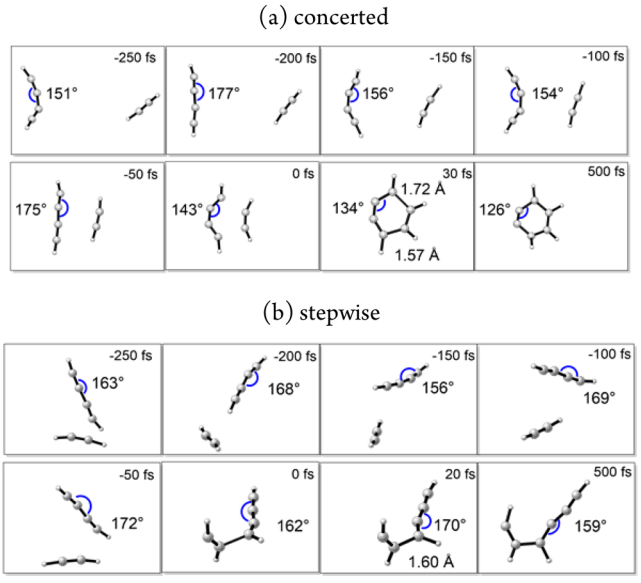

Figure 3. Snapshots for two typical reactive trajectories of butadiyne–acetylene cycloadditions in (a) concerted pathway where butadiyne and acetylene lead to benzyne and in (b) stepwise pathway in which butadiyne and acetylene give a diradical intermediate after one C–C bond formation. The intermediate does not give the benzyne intermediate within 500 fs. Time 0 fs corresponds to the transition state geometry where trajectories are initiated.

before it reaches the transition state. The bending angle of butadiyne is 151° at −250 fs, 177° at −200 fs, 154° at −100 fs, 175° at −50 fs, and 143° at 0 fs. This vibration displays a large bending angle oscillation (~25° oscillation amplitude). The first C–C bond of benzyne forms at 30 fs. We consider bond formation to occur when the first C–C distance reaches 1.6 Å. The time gap between formation of the two bonds is 3 fs. This is a highly dynamically concerted trajectory, since we have defined a dynamically concerted trajectory as one with a time gap of 60 fs or less.[7,42] In comparison, the period of vibration for a fully formed C–C bond is 30 fs.[42]

Figure 3b shows a stepwise trajectory. From −250 to 0 fs, the bending angle ranges from 156° to 172° (~16°). The oscillation pattern of the stepwise trajectory is not as severe as the concerted one. Notably, butadiyne and acetylene mutually rotate as they approach the transition state. The first bond forms at 20 fs, which is comparable to the timing of first bond formation in the concerted pathway. The second bond does not form during the full 500 fs simulation, indicating the formation of a relatively long-lived diradical intermediate.

Results for 300 butadiyne–acetylene cycloaddition molecular dynamics trajectories are summarized in Figure 4. Figure 4a shows the 150 concerted and 150 stepwise trajectories, plotted with respect to two forming bond lengths, Bond 1 and Bond 2 labeled on the graph. Trajectories are initiated from the transition state (blue dots shown on the graph). The 98% confidence interval of the forming bond lengths in the transition state was defined as the transition zone. The transition zones in the concerted trajectories are 2.24 ± 0.29 Å for both bonds, and those in the stepwise trajectories are 5.54 ± 0.32 Å for Bond 1 and 1.80 ± 0.05 Å for Bond 2. The concerted and stepwise trajectories largely overlap on the upper right corner of the graph, (4–6 Å for both bonds), which is the region of separated reactants. The trajectories on the concerted pathway move diagonally on the two-dimensional PES, because

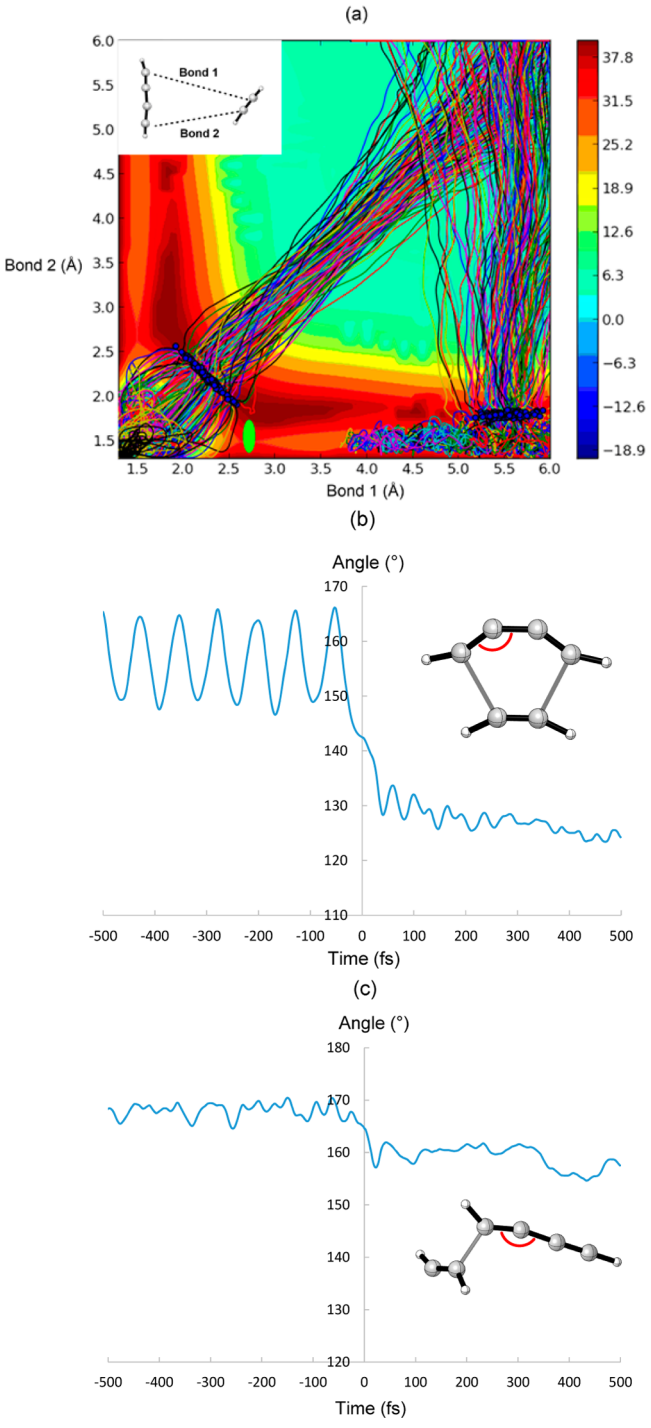

Figure 4. (a) Distribution of 300 reactive trajectories, 150 for the concerted pathway and 150 for the stepwise pathway. Blue dots are starting points from normal mode sampling used to initiate trajectories. Contour plots were calculated with UM06-2X/6-31G(d). Energies are in kcal/mol relative to separated reactants. The energy scale is shown on the right. (b) The averaged trajectory generated from 150 quasiclassical trajectories represented by bending angle versus time in the concerted butadiyne–acetylene reactions. (c) The averaged trajectory generated from 150 quasiclassical trajectories represented by bending angle versus time in the stepwise butadiyne–acetylene reactions. Bending angles are labeled in red on each TS structure.

both bond lengths must decrease together to pass the concerted reaction barrier. The stepwise trajectories move

DOI: 10.1021/jacs.6b04113
J. Am. Chem. Soc. 2016, 138, 8247–8252

vertically, because only Bond 2 forms in crossing the first barrier. Bond 2 is about 1.5 Å in the intermediates, while Bond 1 is 4−6 Å, indicating the random rotation of the newly formed Bond 2. During the time of passage beyond **TS-6s**, only intermediates are formed, and none of the diradicals traverse the second transition state region marked by a green oval in Figure 4a. The intermediate is 5 kcal/mol below the second TS (Table 2, entry 6), and both rotation about Bond 2 and vibrational excitation is required before the second bond can form. This takes picoseconds, not femtoseconds.

Figure 4b shows a single trajectory generated from averaging the 150 trajectories initiated from the concerted butadiyne−acetylene cycloaddition TS. The averaged trajectory shows a strong oscillation pattern from −500 to −50 fs. A concerted single trajectory was conducted to investigate how activation energy is partitioned into translational, rotational, and vibrational motions in reactants.[43,44] The single trajectory was propagated using UM06-2X/6-31G(d) method with no ZPE or thermal energy and with 0.6 kcal/mol kinetic energy in the direction of the reaction coordinate. The 33.9 kcal/mol barrier plus 0.6 kcal/mol kinetic energy is released in these reactants as 15.9 kcal/mol translational energy, 0 kcal/mol rotational energy, and 18.4 kcal/mol vibrational energy.[45] This result shows the bending excitation in the HDDA reactions as the linear diyne reactants distort to form the TS geometries. The oscillation pattern was previously reported in fluoroethane decomposition to hydrofluoride and ethene,[46] 1,2,6-heptatriene rearrangement to 3-methylenehexa-1,5-diene,[47] and several 1,3-dipolar cycloadditions.[43] In these papers, the oscillation was attributed to a significant bending vibrational excitation that must occur in productive trajectories, and this is the case here, as well. After −50 fs, the bending angle of the averaged trajectory decreases to about 130° to form benzyne product. The oscillation amplitude after forming the product largely decreases.

In contrast, the averaged trajectory for the stepwise reaction displayed in Figure 4c does not show a significant oscillation pattern from −500 to 0 fs. Energy partition of the stepwise single trajectory shows that the 32.4 kcal/mol barrier plus 0.6 kcal/mol kinetic energy is partitioned to 14.4 kcal/mol translational energy, 11.2 kcal/mol rotational energy, and 7.5 kcal/mol vibrational energy in the reactants.[45] The stepwise mechanism involves considerable rotational excitation, and a moderate degree of vibrational excitation during the formation of the first C−C bond. A diradical intermediate is formed after the first bond formation, and the intermediate still survives after 500 fs. The chaotic pattern after 0 fs is suggestive of intramolecular vibrational energy relaxation.

CONCLUSION

We report details of the concerted and stepwise mechanisms of six Diels−Alder (DA) and dehydro-Diels−Alder (DDA) reactions. While the stepwise mechanisms have similar barriers for the six prototype reactions studied, the energies of concerted transition states differ significantly in the series. Distortion/interaction analyses reveal that this difference originates from the distortion energy required to achieve the transition states. One manifestation of this distortion-controlled reactivity of DDA reactions is that the stepwise HDDA reaction is competitive with the concerted mechanism.

Direct molecular dynamics (MD) simulations for the concerted and stepwise mechanisms of the HDDA reaction were conducted. From −500 to 0 fs, the concerted trajectories display a strong bending angle oscillation (~25° oscillation amplitude), while the stepwise trajectories show a relatively chaotic pattern, and rotational motion instead. The concerted mechanism of the HDDA reaction involves high bending vibrational excitation, because linear diyne reactants need to be highly bent to form the TS geometries. In contrast, the stepwise mechanism requires less geometrical deformation to enable the first C−C bond formation.

The distortion/interaction analyses, based upon the transition structures computed for each reaction, reflect the observations from MD trajectory simulations. That is, the more highly distorted the transition state, the greater the necessity for excitation of the corresponding vibrational modes in order to achieve productive trajectories.

ASSOCIATED CONTENT

Supporting Information

The Supporting Information is available free of charge on the ACS Publications website at DOI: 10.1021/jacs.6b04113.

Results for transition state normal model sampling in the gas phase, single trajectory energy partition, input parameters for Progdyn, and coordinates and energies of stationary points (PDF)

Movie of reactive trajectory shown in Figure 3a (MPG)

Movie of reactive trajectory shown in Figure 3b (MPG)

AUTHOR INFORMATION

Corresponding Author

*houk@chem.ucla.edu

Author Contributions

†P.Y. and Z.Y contributed equally.

Notes

The authors declare no competing financial interest.

ACKNOWLEDGMENTS

We thank Dr. Charles Doubleday for the program to perform the single trajectory energy partition. This work was supported by the National Science Foundation (Grant CHE-1361104). Calculations were performed on the Hoffman2 cluster at UCLA and the Extreme Science and Engineering Discovery Environment (XSEDE), which is supported by the National Science Foundation (Grant OCI-1053575).

REFERENCES

(1) Diels, O.; Alder, K. *Justus Liebigs Annalen der Chemie* **1928**, *460*, 98.

(2) Norton, J. A. *Chem. Rev.* **1942**, *31*, 319.

(3) Martin, J. G.; Hill, R. K. *Chem. Rev.* **1961**, *61*, 537.

(4) Winkler, J. D. *Chem. Rev.* **1996**, *96*, 167.

(5) Nicolaou, K. C.; Snyder, S. A.; Montagnon, T.; Vassilikogiannakis, G. *Angew. Chem., Int. Ed.* **2002**, *41*, 1668.

(6) Goldstein, E.; Beno, B.; Houk, K. N. *J. Am. Chem. Soc.* **1996**, *118*, 6036.

(7) Black, K.; Liu, P.; Xu, L.; Doubleday, C.; Houk, K. N. *Proc. Natl. Acad. Sci. U. S. A.* **2012**, *109*, 12860.

(8) Hoffmann, R.; Woodward, R. B. *J. Am. Chem. Soc.* **1965**, *87*, 4388.

(9) Kagan, H. B.; Riant, O. *Chem. Rev.* **1992**, *92*, 1007.

(10) Funel, J.-A.; Abele, S. *Angew. Chem., Int. Ed.* **2013**, *52*, 3822.

(11) Brieger, G.; Bennett, J. N. *Chem. Rev.* **1980**, *80*, 63.

(12) Juhl, M.; Tanner, D. *Chem. Soc. Rev.* **2009**, *38*, 2983.

(13) Marsault, E.; Toró, A.; Nowak, P.; Deslongchamps, P. *Tetrahedron* **2001**, *57*, 4243.

DOI: 10.1021/jacs.6b04113
J. Am. Chem. Soc. 2016, 138, 8247−8252

(14) (a) Yu, P.; Patel, A.; Houk, K. N. *J. Am. Chem. Soc.* **2015**, *137*, 13518. (b) He, C. Q.; Chen, T. Q.; Patel, A.; Karabiyikloglu, S.; Merlic, C. A.; Houk, K. N. *J. Org. Chem.* **2015**, *80*, 11039.
(15) Maruoka, K.; Itoh, T.; Shirasaka, T.; Yamamoto, H. *J. Am. Chem. Soc.* **1988**, *110*, 310.
(16) Jørgensen, K. A. *Angew. Chem., Int. Ed.* **2000**, *39*, 3558.
(17) Blackman, M. L.; Royzen, M.; Fox, J. M. *J. Am. Chem. Soc.* **2008**, *130*, 13518.
(18) Devaraj, N. K.; Weissleder, R.; Hilderbrand, S. A. *Bioconjugate Chem.* **2008**, *19*, 2297.
(19) (a) Yang, J.; Šečkutė, J.; Cole, C. M.; Devaraj, N. K. *Angew. Chem., Int. Ed.* **2012**, *51*, 7476. (b) Patterson, D. M.; Nazarova, L. A.; Xie, B.; Kamber, D. N.; Prescher, J. A. *J. Am. Chem. Soc.* **2012**, *134*, 18638.
(20) Jiang, X.; Wang, R. *Chem. Rev.* **2013**, *113*, 5515.
(21) Kim, H. J.; Ruszczycky, M. W.; Choi, S.-H.; Liu, Y.-N.; Liu, H.-W. *Nature* **2011**, *473*, 109.
(22) Tian, Z.; Sun, P.; Yan, Y.; Wu, Z.; Zheng, Q.; Zhou, S.; Zhang, H.; Yu, F.; Jia, X.; Chen, D.; Mandi, A.; Kurtan, T.; Liu, W. *Nat. Chem. Biol.* **2015**, *11*, 259.
(23) Klas, K.; Tsukamoto, S.; Sherman, D. H.; Williams, R. M. *J. Org. Chem.* **2015**, *80*, 11672.
(24) Wessig, P.; Müller, G. *Chem. Rev.* **2008**, *108*, 2051.
(25) A term "dehydropericyclic" has been used to describle the analogous variants of the more general pericyclic reactions. (a) Johnson, R. P. *J. Phys. Org. Chem.* **2010**, *23*, 283. (b) Skraba-Joiner, S.; Johnson, R. P.; Agarwal, J. *J. Org. Chem.* **2015**, *80*, 11779.
(26) Wessig, P.; Müller, G.; Herre, R.; Kühn, A. *Helv. Chim. Acta* **2006**, *89*, 2694.
(27) Kocsis, L. S.; Kagalwala, H. N.; Mutto, S.; Godugu, B.; Bernhard, S.; Tantillo, D. J.; Brummond, K. M. *J. Org. Chem.* **2015**, *80*, 11686.
(28) Brummond, K. M.; Kocsis, L. S. *Acc. Chem. Res.* **2015**, *48*, 2320.
(29) Li, W.; Zhou, L.; Zhang, J. *Chem. - Eur. J.* **2016**, *22*, 1558.
(30) (a) Hoye, T. R.; Baire, B.; Niu, D.; Willoughby, P. H.; Woods, B. P. *Nature* **2012**, *490*, 208. (b) Yun, S. Y.; Wang, K.-P.; Lee, N.-K.; Mamidipalli, P.; Lee, D. *J. Am. Chem. Soc.* **2013**, *135*, 4668. For earlier reports of this reaction, see: (c) Bradley, A. Z.; Johnson, R. P. *J. Am. Chem. Soc.* **1997**, *119*, 9917. (d) Miyawaki, K.; Suzuki, R.; Kawano, T.; Ueda, I. *Tetrahedron Lett.* **1997**, *38*, 3943. For a review, see: (e) Holden née Hall, C.; Greaney, M. F. *Angew. Chem., Int. Ed.* **2014**, *53*, 5746.
(31) Hoffmann, R.; Woodward, R. B. *J. Am. Chem. Soc.* **1965**, *87*, 2046.
(32) Zhang, X.; Maccarone, A. T.; Nimlos, M. R.; Kato, S.; Bierbaum, V. M.; Ellison, G. B.; Ruscic, B.; Simmonett, A. C.; Allen, W. D.; Schaefer, H. F. *J. Chem. Phys.* **2007**, *126*, 044312.
(33) Ajaz, A.; Bradley, A. Z.; Burrell, R. C.; Li, W. H. H.; Daoust, K. J.; Bovee, L. B.; DiRico, K. J.; Johnson, R. P. *J. Org. Chem.* **2011**, *76*, 9320.
(34) Marell, D. J.; Furan, L. R.; Woods, B. P.; Lei, X.; Bendelsmith, A. J.; Cramer, C. J.; Hoye, T. R.; Kuwata, K. T. *J. Org. Chem.* **2015**, *80*, 11744.
(35) Liang, Y.; Hong, X.; Yu, P.; Houk, K. N. *Org. Lett.* **2014**, *16*, 5702.
(36) Wang, T.; Naredla, R. R.; Thompson, S. K.; Hoye, T. R. *Nature* **2016**, *532*, 484.
(37) Frisch, M. J.; Trucks, G. W.; Schlegel, H. B.; Scuseria, G. E.; Robb, M. A.; Cheeseman, J. R.; Scalmani, G.; Barone, V.; Mennucci, B.; Petersson, G. A.; Nakatsuji, H.; Caricato, M.; Li, X.; Hratchian, H. P.; Izmaylov, A. F.; Bloino, J.; Zheng, G.; Sonnenberg, J. L.; Hada, M.; Ehara, M.; Toyota, K.; Fukuda, R.; Hasegawa, J.; Ishida, M.; Nakajima, T.; Honda, Y.; Kitao, O.; Nakai, H.; Vreven, T.; Montgomery, J. A., Jr.; Peralta, J. E.; Ogliaro, F.; Bearpark, M.; Heyd, J. J.; Brothers, E.; Kudin, K. N.; Staroverov, V. N.; Kobayashi, R.; Normand, J.; Raghavachari, K.; Rendell, A.; Burant, J. C.; Iyengar, S. S.; Tomasi, J.; Cossi, M.; Rega, N.; Millam, J. M.; Klene, M.; Knox, J. E.; Cross, J. B.; Bakken, V.; Adamo, C.; Jaramillo, J.; Gomperts, R.; Stratmann, R. E.; Yazyev, O.; Austin, A. J.; Cammi, R.; Pomelli, C.; Ochterski, J. W.; Martin, R. L.; Morokuma, K.; Zakrzewski, V. G.; Voth, G. A.; Salvador, P.; Dannenberg, J. J.; Dapprich, S.; Daniels, A. D.; Farkas, O.; Foresman, J. B.; Ortiz, J. V.; Cioslowski, J.; Fox, D. J. *Gaussian 09*, revision D.01; Gaussian, Inc.: Wallingford, CT, 2013.
(38) (a) Zhao, Y.; Truhlar, D. G. *Theor. Chem. Acc.* **2008**, *120*, 215. (b) Zhao, Y.; Truhlar, D. G. *Acc. Chem. Res.* **2008**, *41*, 157.
(39) Singleton, D. A.; Wang, Z. H. *J. Am. Chem. Soc.* **2005**, *127*, 6679.
(40) (a) Ess, D. H.; Houk, K. N. *J. Am. Chem. Soc.* **2007**, *129*, 10646. (b) Ess, D. H.; Houk, K. N. *J. Am. Chem. Soc.* **2008**, *130*, 10187. The distortion/interaction model has been used to study the machanism and reactivity of a variety of cycloaddtion reactions. For relevant studies, see: (c) Liu, S.; Lei, Y.; Qi, X.; Lan, Y. *J. Phys. Chem. A* **2014**, *118*, 2638. (d) Qi, X.; Li, Y.; Zhang, G.; Li, Y.; Lei, A.; Liu, C.; Lan, Y. *Dalton Trans.* **2015**, *44*, 11165. (e) Li, Y.; Qi, X.; Lei, Y.; Lan, Y. *RSC Adv.* **2015**, *5*, 49802.
(41) (a) van Zeist, W.-J.; Bickelhaupt, F. M. *Org. Biomol. Chem.* **2010**, *8*, 3118. (b) Fernández, I.; Bickelhaupt, F. M. *Chem. Soc. Rev.* **2014**, *43*, 4953.
(42) (a) Xu, L.; Doubleday, C. E.; Houk, K. N. *J. Am. Chem. Soc.* **2011**, *133*, 17848. (b) Yang, Z.; Yu, P.; Houk, K. N. *J. Am. Chem. Soc.* **2016**, *138*, 4237. (c) Patel, A.; Chen, Z.; Yang, Z.; Gutiérrez, O.; Liu, H.-w.; Houk, K. N.; Singleton, D. A. *J. Am. Chem. Soc.* **2016**, *138*, 3631. (d) Yang, Z.; Doubleday, C.; Houk, K. N. *J. Chem. Theory Comput.* **2015**, *11*, 5606. (e) Hong, X.; Bercovici, D. A.; Yang, Z.; Al-Bataineh, N.; Srinivasan, R.; Dhakal, R. C.; Houk, K. N.; Brewer, M. *J. Am. Chem. Soc.* **2015**, *137*, 9100. (f) Liu, F.; Yang, Z.; Mei, Y.; Houk, K. N. *J. Phys. Chem. B* **2016**, DOI: 10.1021/acs.jpcb.6b02336.
(43) Xu, L.; Doubleday, C. E.; Houk, K. N. *J. Am. Chem. Soc.* **2010**, *132*, 3029.
(44) Raff, L. M. *J. Chem. Phys.* **1988**, *89*, 5680.
(45) The energy partition of single trajectory is detailed in the Supporting Information. The partition energies in reactants are averaged over 1000 fs in single trajectory after the reactants are separated by 5 Å. The error in average partition energy is about 0.2 kcal/mol, which causes the slight difference between the energy barrier and the sum of partition energies in the reactants.
(46) Sun, L.; Park, K.; Song, K.; Setser, D. W.; Hase, W. L. *J. Chem. Phys.* **2006**, *124*, 064313.
(47) Debbert, S. L.; Carpenter, B. K.; Hrovat, D. A.; Borden, W. T. *J. Am. Chem. Soc.* **2002**, *124*, 7896.

DOI: 10.1021/jacs.6b04113
J. Am. Chem. Soc. 2016, 138, 8247−8252